

# Batch Polymerization of Methyl Methacrylate in Mini/Macroemulsions

K. FONTENOT and F. J. SCHORK\*

Georgia Institute of Technology, School of Chemical Engineering, Atlanta, Georgia 30332-0100

## SYNOPSIS

The kinetics of the isothermal batch macroemulsion and miniemulsion polymerizations of methyl methacrylate (MMA) at 50°C have been studied. Hexadecane was used as the cosurfactant or swelling agent. The nucleation mechanisms were observed to be different between macroemulsions and miniemulsions. The effect of surfactant, cosurfactant, initiator, shear, and hold time on droplet nucleation was studied. The miniemulsion particles were found to contain more radicals on average than the macroemulsion particles using certain recipes. This resulted in higher polymerization rates for the miniemulsions at identical particle numbers. The latex particle-size distributions were similar even though the miniemulsion droplets start out with a high polydispersity of around 1.5. Miniemulsion latexes were found to be more stable under shear. Conductance of emulsions during polymerization was found to be a valuable on-line tool for investigating particle nucleation and growth.

© 1993 John Wiley & Sons, Inc.

## 1. INTRODUCTION

The term macroemulsion is used here to distinguish the conventional emulsion from emulsions in general, which can be macro-, mini-, or microemulsions. Macroemulsions do not use cosurfactants and have monomer droplets with diameters on the order of 1–10 microns, whereas miniemulsions use cosurfactants or swelling agents to provide stability to sub-micron monomer droplets, thereby reducing the average size to 0.1–0.5 microns. Ostwald ripening (transfer of monomer from small droplets to large droplets to reduce the total surface energy of the system) results in the increase of the average droplet diameter in an emulsion. This, along with coalescence and settling, are the mechanisms by which emulsions break. A swelling agent is very water insoluble and prohibits the complete diffusion of monomer from the small droplets, thus slowing down the emulsion breakdown process.

Both miniemulsions and macroemulsions polymerize under reaction conditions. Initiators may be either water- or oil-soluble. Miniemulsion polymer-

izations are relatively new; they have only been around since the early 1970s. Miniemulsion polymerizations follow a different mechanism from macroemulsion polymerizations. Nucleation of monomer droplets leads to a different mechanism from macroemulsion polymerizations. Nucleation of monomer droplets leads to a different rate of polymerization and a different final product. It is important to quantify these differences since miniemulsions are a relatively new development. In addition, since droplet nucleation occurs in macroemulsion polymerizations, these studies can also aid in the understanding of conventional emulsion polymerization. Miniemulsions still follow typical Smith and Ewart (SE)<sup>1</sup> kinetics and are not simply “small” versions of suspension polymerizations.

The literature provides examples of miniemulsion polymerizations in both batch and continuous reactors.<sup>2–5</sup> Miniemulsion copolymerizations have also been performed.<sup>6</sup> Initiators have been both oil-based and aqueous-based.<sup>7</sup> Miniemulsion polymerizations in seeded systems have also been studied.<sup>7–9</sup> However, little has been done in determining the effect shear or droplet size has on polymerizations. By carrying out these polymerizations at various reaction recipes, one can clarify the importance of these effects as well as verify the utility of a model<sup>10</sup> in

\* To whom correspondence should be addressed.

predicting particle number and polymerization rates. Both miniemulsion and macroemulsion systems are considered to allow direct comparison of the two.

Some important factors to evaluate through polymerization of mini/macroemulsions include

- The effect of surfactant, cosurfactant, shear, and percent organic phase on the locus of particle nucleation.
- The effect of surfactant, cosurfactant, and initiator on particle number for both miniemulsion and macroemulsion polymerizations.
- The reproducibility of droplet nucleation.
- The differences in the gel and glass effects between miniemulsion and macroemulsion polymerizations.
- The effect of nucleation locus on particle-size distribution and molecular weight distribution.
- The shear stability of the final latex.
- The fluctuations in surface tension or conductance during polymerization corresponding to shifts in surface active agents and/or the presence of micelles.

These areas all become important when working with the wide range of emulsion systems as one goes from macroemulsions to miniemulsions.

## 2. EXPERIMENTAL

### 2.1. Reagents

The following materials were used in the batch polymerization of methyl methacrylate (MMA) at 50°C. MMA was chosen because of its large gel effect, its slight water solubility, its stability as a miniemulsion, and the copious amounts of data available on MMA constants and polymerizations:

- Methyl methacrylate (MMA),  $\{\text{CH}_2=\text{C}(\text{CH}_3)\text{CO}_2\text{CH}_3\}$  (MW = 100.13), inhibited, supplied by Rohm and Haas. The inhibitor (methylethyl hydroquinone, 10 ppm) was removed by vacuum distillation at 35–40°C prior to use. Purified MMA was stored at 5°C until needed.
- Sodium dodecyl sulfate (SLS),  $\{\text{C}_{12}\text{H}_{25}\text{OSO}_3\cdot\text{Na}\}$  (MW = 288.38), 99% specially pure, supplied by BDH Limited, Poole, England (available in the U.S. through Gallard Schlesinger Chemicals Manufacturing Co., Carle Place, NY), was used as supplied. Surface ten-

sion measurements revealed no dip at the CMC, which would indicate impurities. The value of the CMC at room temperature (20°C) in pure water was found through conductance measurements to be  $7.4 \pm 0.15$  mmol/L aq. The value at 50°C in water saturated with MMA was measured to be  $6.70 \pm 0.30$  mmol/L aq. The ranges given are 95% confidence intervals about the estimates for the CMC.

- Water was deionized (DI) prior to use (conductance measured to be  $< 3.0 \mu\text{S}/\text{cm}$ ).
- All other chemicals were used as received.

### 2.2. Apparatus

The reaction vessel with associated equipment has been presented earlier,<sup>11</sup> as has the procedure in extensive detail. The device used to provide high intensity shear in the breakup of monomer droplets was the Fisher 300W Sonic Dismembrator. The emulsification/polymerization procedure is listed here in brief for completeness.

Regardless of the recipe employed, the polymerization procedure followed was standard. The procedure for miniemulsion polymerizations varies from that for macroemulsions. Both are listed below. The "standard recipe" refers to the following 30% organic phase reaction conditions:

- 510 g DI water
- 220 g MMA
- 5 g hexadecane HD = 0.0232 g/g MMA (mini-emulsions only)

**Table I** Cross Listing of Recipe Conditions with Run Numbers for MMA Macroemulsion Polymerizations

Soap (mol/L)	Initiator (mol/L)				
	0.001	0.002	0.005	0.010	0.020
0.005			26		
0.007			22		
0.0093			21		
0.012			24		
0.020	19	17	11	8, 10, 97	18
0.030			30		
0.040		103	20, 39, 93	100	
0.070			25		
0.100			23		
0.130			27		

Base Conditions: 510 g H<sub>2</sub>O; 220 g MMA; 50°C, 1 L reactor, 400 rpm stirring. Conditions not shown are as in standard recipe.

- 0.02 mol SLS/L H<sub>2</sub>O = 2.942 g
- 0.005 mol K<sub>2</sub>S<sub>2</sub>O<sub>8</sub>/L H<sub>2</sub>O = 0.6894 g
- 50°C reaction temperature
- 400 ± 20 rpm stirrer speed
- 5 min of preshear at 2200 ± 100 rpm (mini-emulsions only)
- 6 min of sonication at 60% energy load (mini-emulsions only).

The recipes employed were usually a version of this recipe. Differences are pointed out where appropriate. Tables I and II provide a listing of the polymerizations performed for MMA macroemulsions and miniemulsions, respectively. The run numbers are listed for cross-referencing.

### 2.3. Macroemulsion Polymerizations

The reactor was assembled and the condenser cooling water and reactor nitrogen purge were initiated. A leak check of the apparatus verified that a closed system existed. The reactor was then inventoried stepwise. The required amount of surfactant was

added to the reactor. The desired amount of DI water (recipe amount less that needed to dissolve initiator) was added to the reactor and stirring was begun. Nitrogen sparging was maintained a minimum of 15 min. Once this was completed, the measured amount of MMA was added to the reactor. Nitrogen flow was slightly reduced to minimize evaporation of MMA. Stirring and purging were maintained for an additional 15 min.

The reaction was initiated in the following sequence: The nitrogen purge was reduced to a minimal flow of approximately 5 mL per min. The stirring rate was reduced to 400 ± 20 rpm. The temperature controller was activated and the desired temperature set. As the reactor temperature increased to the setpoint, the initiator was dissolved in the remaining DI water. When the temperature reached the setpoint (about 5 min), the reaction was started by injecting the initiator solution. The reactor temperature was monitored during the exothermic portion of the reaction so that cooling water could be activated manually to the internal cooling coil, if needed. Control was typically within 1°C.

**Table II Cross Listing of Recipe Conditions with Run Numbers for MMA Miniemulsion Polymerizations**

Soap (mol/L)	HD (g) ⇒ ↓ SONIC (min)	Initiator (mol/L)								
		0.001	0.002	0.005		0.010	0.020	0.040		
		5	5	2	5	10	21	5	5	5
0.008	6				63					
0.010	2				90					
	6			68	61	70		51		
	12				83					
0.020	2				91			86		
	4				84			85		
	6				57			49		
		58	65	66	98	50		55	53	54
					101			102		
		8					77	82		
0.040	12				72			52	78	
	2							88		
	4				87					
	6			67						
				71	62	69		99		
0.080				89						
	12				79					
	6				64					

Base Conditions: 510 g H<sub>2</sub>O, 220 g MMA, 50°C, 400 rpm stirring, 1 L reactor, 5 min preshear, sonicate at 60%, 30 min hold time. Conditions not shown are as in the standard recipe.

Samples were taken by removal of approximately 10 g of latex from the reactor and short-stopping the reaction by injection into a vial containing hydroquinone solution. Conversions were determined gravimetrically. Particle sizes were measured with a Malvern IIc Autosizer.

#### 2.4. Miniemulsion Polymerizations

The procedure for preparation of the miniemulsions required additional steps. The recipe amount of DI water (less that needed for dissolving initiator) was added to the reactor bell. Stirring sufficient to pull a vortex was begun. The recipe amount of surfactant was added and allowed to dissolve in the water (about 10 min). A homogeneous mixture containing the desired amounts of MMA and HD was added to the aqueous solution in the reactor. The mixture was stirred magnetically for 15 min to allow equilibration.

After dispersing the monomer in the aqueous solution, the mixture was sheared with a slotted disc paddle at  $2200 \pm 100$  rpm for 5 min to reduce the monomer droplets to a size that was more efficiently sheared by sonication. Sonication was then performed for the desired amount of time with the sonic dismembrator while a magnetic stirrer provided bulk mixing.

Upon completion of sonication, the probe and stirrer were removed and the reactor head with condenser and coils was installed. The nitrogen purge and cooling water were activated to purge oxygen from the reactor system. After 30 min of purge, the setpoint of the temperature controller was raised to the desired temperature and the reactor heated up. Once a steady temperature was reached, the polymerization was started by addition of the initiator. The sampling and analysis were identical to that described in the macroemulsion section.

One note regarding the conversion calculation should be made: Although HD has a normal boiling point of  $287^\circ\text{C}$ , it was found to evaporate in a  $65\text{--}75^\circ\text{C}$  oven. For this reason, conversion calculations assumed that no HD is left in the miniemulsion samples once they had dried overnight. This assumption was found to be less valid at the higher conversions where polymer kept the HD from evaporating.

#### 2.5. Particle Sizes

Particle-size measurements were performed by two methods: A sample of the latex was diluted 100–500-fold (depending on the conversion) with SLS in DI solution to obtain the desired translucence.

The concentration of SLS was kept around 0.001 mol/L aqueous. If the conversion of the sample was greater than 70%, no further work was required and measurements were made on the Malvern IIc Autosizer. For conversion greater than 70%, it was assumed that any residual monomer was eluted to the aqueous phase upon dilution. Usually 6–10 light-scattering measurements were taken to determine reproducibility and confidence.

If the conversion was less than 70%, the diluted sample was placed in a  $70^\circ\text{C}$  oven for several hours to drive off the excess monomer. The mixture was then allowed to cool prior to making light-scattering measurements. Runs were repeated here as well. All Malvern IIc measurements were obtained at  $25^\circ\text{C}$ .

Particle numbers and concentrations were determined from the calculated conversion and the measured average particle diameter. The equation used is of the form

$$N_p = \hat{N}_p / V_R \\ = \frac{1}{V_R} \frac{6 (\% \text{ conversion})(\text{mass monomer})}{\pi \bar{d}_p^3 \rho_p} \quad (1)$$

where  $V_R$  is the volume of the reactor contents;  $\hat{N}_p$ , the number of particles;  $N_p$ , the concentration of particles;  $\rho_p$ , the density of polymer; and  $\bar{d}_p$ , the volume-average diameter (or root mean cube [RMC]) of the particles. Propagation of error in the percent conversion, particle diameters, and reactant volumes gives the error limits for the particle number or concentration. The volume-average diameter is calculated from the particle size number distribution as

$$\bar{d}_p = \left( \frac{\sum d_i^3 N_{pi}}{\sum N_{pi}} \right)^{1/3} \quad (2)$$

Transmission electron microscope (TEM) pictures were also taken of some of the latexes. These pictures provided good indications of secondary nucleation and broad particle-size distributions. However, due to the ease of degradation of MMA in the electron beam, the results were found to be consistently lower than the light-scattering measurement. Time and expense also prohibited the evaluation of all particle-size distributions by this method.

### 3. RESULTS AND DISCUSSION

#### 3.1. Particle Nucleation

The locus of particle nucleation is different between mini- and macroemulsion polymerizations. There is

also a difference in the rate of nucleation of particles. Miniemulsion particles start out as droplets in the 100 nm range, whereas macroemulsion particles start out as micelles (at least at these surfactant levels). Micelles are 3–6 nm in diameter. The radical capture constant is much different between these two systems.

By measuring the particle size throughout the polymerization and calculating the corresponding particle numbers, it is possible to estimate the end of Interval I. Evidence for secondary nucleation can also be obtained. The particle number concentrations during polymerization of four macroemulsions are shown in Figure 1. At the higher concentrations of surfactant (SLS), there is evidence for secondary nucleation near the end of the run. This is most likely a combined effect of particle shrinkage and stabilization by initiator end groups. For this reason, the particle number used in all subsequent calculations is that measured in the plateau region of the curve near 50% conversion. TEM pictures also provided evidence of this secondary nucleation.

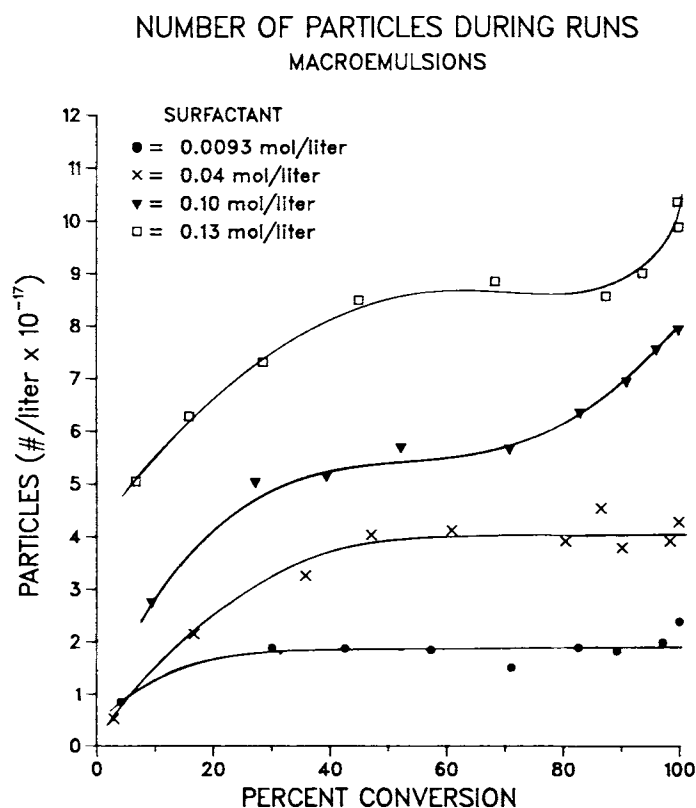
Although the calculations at low conversions are prone to large amounts of error, the data do suggest

that particle nucleation lasts longer (in terms of conversion) for systems with higher surfactant concentrations. The data agree with what has been found in the literature. Particle nucleation in macroemulsions been shown experimentally to last until 10–30% conversion.<sup>12</sup>

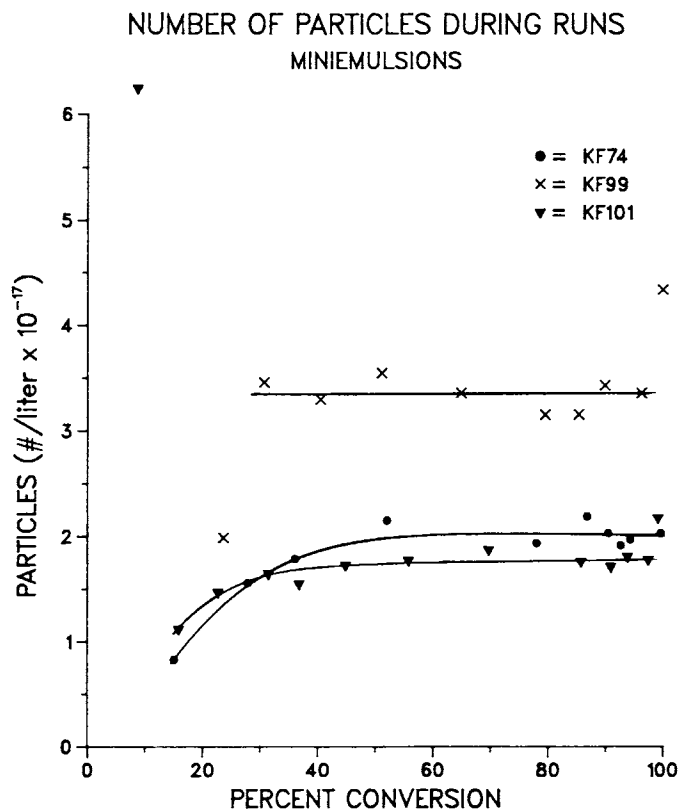
The corresponding curve for miniemulsion polymerizations is given as Figure 2. Obtaining reliable data over the entire range of conversions was more difficult with miniemulsions. This could be a reflection on the origin of these particles. The data again show that nucleation of particles ends at 10–30%. This agrees with the results presented in the literature for the miniemulsion polymerization of styrene.<sup>3</sup>

### 3.2. Effect of Surfactant

According to the SE theory,<sup>1</sup> the particle number concentration is proportional to the surfactant concentration to the 0.6 power. However, data have been reported by many authors that give different values for this proportionality for various monomers. Radical desorption and monomer water solubility are



**Figure 1** Particle number concentrations during macroemulsion polymerization of MMA at 50°C and at four different levels of surfactant. Recipes are standard except for surfactant concentrations. Run numbers are (●) KF21, (×) KF20, (▼) KF23, and (□) KF27.



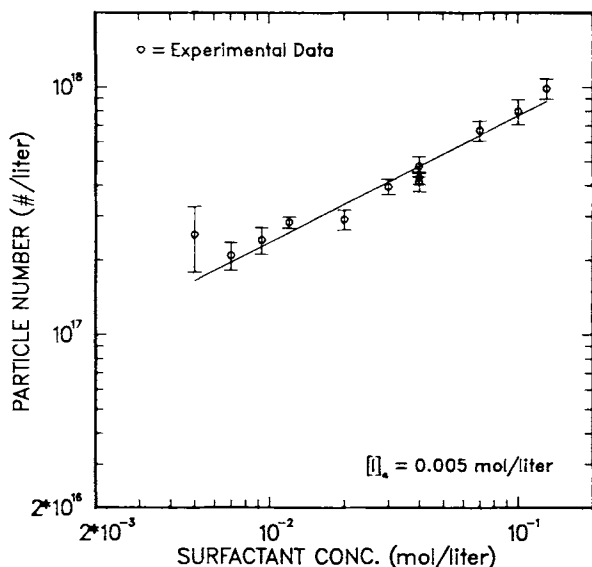
**Figure 2** Particle number concentrations during miniemulsion polymerization of MMA at three different recipe conditions. Recipes are KF74 = standard with  $[I]_a = 0.01$  mol/L  $H_2O$ , 8 min of sonication, and hold time = 70 min; KF99 = standard with  $[S]_a = 0.04$  mol/L  $H_2O$  and  $[I]_a = 0.01$  mol/L  $H_2O$ ; KF101 = standard recipe.

known to influence the value. For MMA, the values range from 0.50 to 3.87.<sup>12-17</sup> The data obtained in this work provide another point. Figure 3 shows the particle numbers obtained experimentally for macroemulsion polymerization of MMA with various levels of surfactant. All conditions except for surfactant concentration are as in the standard recipe. The run numbers corresponding to these data points are presented in Table I.

The line shown on the graph is the linear least-squares fit to the data on the log-log scale. The slope of this line was found to be  $0.51 \pm 0.10$ , which falls within the range of the other data. The range given is the 98% confidence interval about the estimate for the slope. This level of confidence is used as standard throughout unless otherwise specified. The reason for the large range of values reported in the literature is that the functionality of  $N_p$  to  $[S]$  is not actually linear on the log-log scale. Only for certain ranges in surfactant concentrations will linearity hold. As surfactant concentration is decreased, the CMC is approached and the number of particles

created drastically decreases. This is reflected in the shift in nucleation mechanism from micellar to homogeneous. Hansen and Ugelstad<sup>15,18</sup> reported the true appearance of the curve for several monomers over large ranges of surfactant. The slope is therefore an indication of where the polymerizations fall in terms of nucleation. It is, however, useful for comparison of macroemulsion polymerizations to miniemulsions polymerizations.

Miniemulsions are usually created with recipes that have surfactant concentrations that are much higher than the CMC. This would place them on the linear portion of the  $N_p$  vs.  $[S]$  curve. However, the existence of micelles is not only a function of surfactant concentration but also of monomer droplet diameter. Micelles are thought to exist only if the surface area of the free surfactant (that which is in excess of the CMC) is greater than the total droplet surface area. This is preferably not the case in miniemulsions. To avoid bimodal nucleation, a limited amount of surfactant should be used. In certain recipes, an excess of surfactant will result in

PARTICLE NUMBER DEPENDENCE ON SURFACTANT  
 MACROEMULSIONS


**Figure 3** Particle number concentration in different MMA macroemulsion polymerizations at 50°C. Recipes are standard except for surfactant. The solid line is the LLS fit to the data. Run numbers corresponding to these data points are given in Table I. Error bars are 98% confidence intervals about data points as determined from variances in particle-size measurements.

formation of two particle types. It is hard to control the ratio of particle numbers if bimodal nucleation does occur. This is due to the steepness in the rate at which micelles appear.

In miniemulsions, the droplets are not saturated with surfactant. Table III shows the percent surface coverage of droplets of various size by surfactant. The calculations are for a 30% organic emulsion at 50°C where the dissolved monomer and the surfactant have been subtracted out to obtain that available for droplet formation and surface coverage, respectively. Instead of using an isotherm calculation, the calculations assume that surfactant saturates the aqueous phase prior to adsorption on the droplet surface.

Since the surfactant plays a role in determining the droplet diameter in miniemulsions, it also affects the particle number and rate of polymerization. However, unlike macroemulsions, there are many variables other than surfactant concentration that can affect droplet size. These include amount of cosurfactant, amount of shear, and time of nitrogen purge (hold time). For this reason, it is possible to find several curves for the  $N_p$  vs.  $[S]$  relationship.

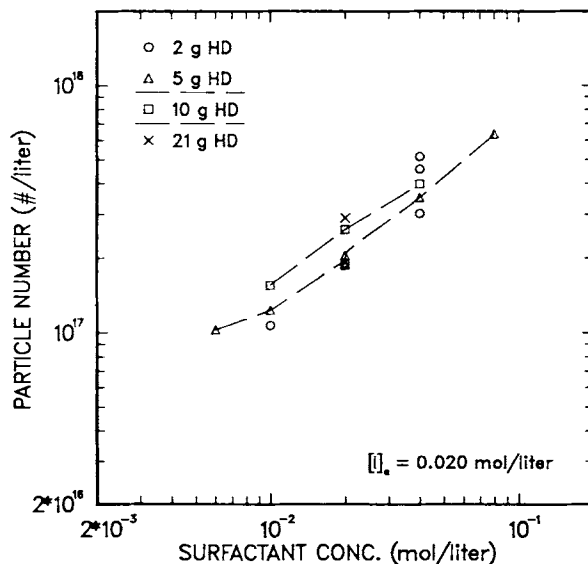
**Table III** Percent Droplet Surface Coverage by Surfactant in 30% MMA Miniemulsions at 50°C

Surfactant (mol/L)	Droplet Diameter		
	100 nm	150 nm	200 nm
0.01	8.1%	12.1%	16.1%
0.02	20.7%	31.0%	41.3%
0.04	45.9%	68.8%	91.8%

Droplets are assumed to be monodisperse at indicated diameters. Various levels of surfactant are used.

Figure 4 gives three such curves for various levels of cosurfactant. The slopes of these lines appear to be equal. Statistically, there is no difference. If it is assumed they are equal, the average slope of the lines is found to be  $0.77 \pm 0.13$ , which is much higher than that measured for macroemulsions. If both micellar and droplet nucleation occurred at the higher levels of surfactant and low levels of HD, this value number could be inflated.

Delgado found different results for the copolymerization of vinyl acetate and butyl acrylate<sup>19</sup> with sodium hexadecyl sulfate (SHS) as surfactant and

 PARTICLE NUMBER DEPENDENCE ON SURFACTANT  
 MINIEMULSIONS


**Figure 4** Particle number concentration in different miniemulsion polymerizations of MMA at 50°C. Recipes are standard except for variations in the levels of surfactant and cosurfactant. Run numbers for these data points are given in Table II.

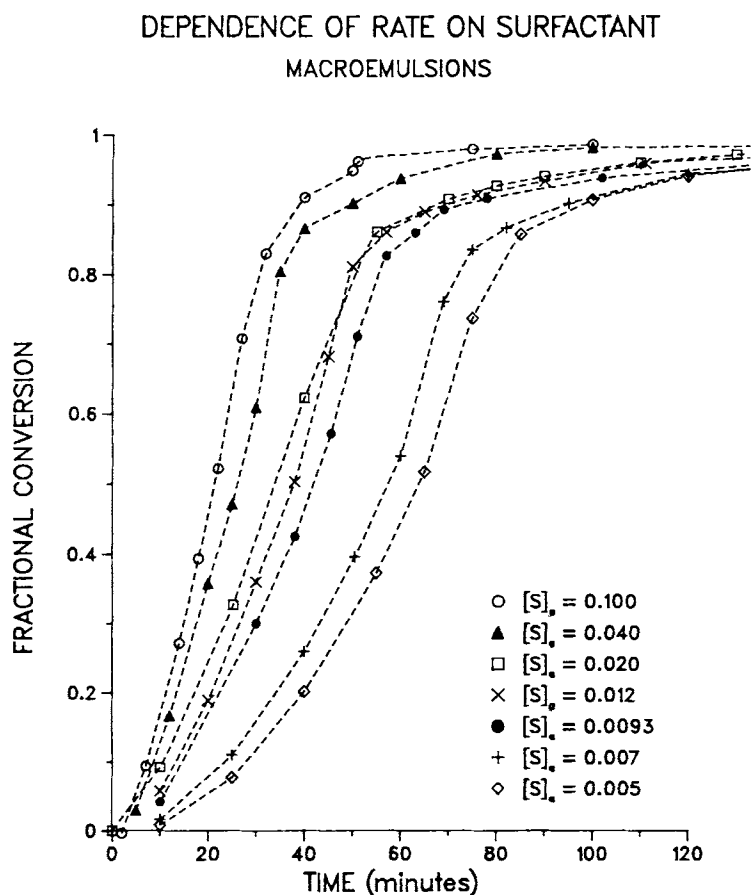
HD as cosurfactant. The macroemulsion polymerizations had a slope of 0.68 on the  $N_p$  vs.  $[S]$  log-log curve. The miniemulsions had a lower slope at 0.25. However, both the concentration used and the CMC of SHS are an order of magnitude smaller than in this work. The type or amount of shear will also play a role since more sonication usually means more droplets. This is discussed in a later section.

The conversion time curves for some of the data points in Figures 3 and 4 are shown in Figure 5 for the macroemulsions and in Figure 6 for the miniemulsions. The rate of polymerization correlates well with the number of particles for both miniemulsion and macroemulsion polymerizations. There are differences in the shape of these curves due to different gel and glass effects as well as differences in the kinetics.

Miniemulsion latex particles have an origin different from macroemulsion particles. This leads to a far different monomer concentration within the

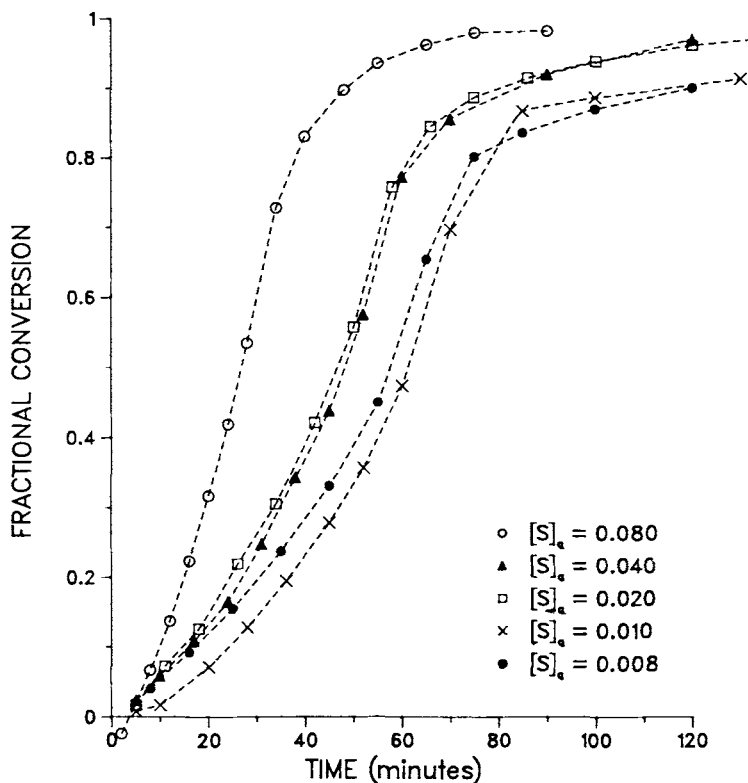
particle over the course of the reaction. Macroemulsion particles are normally assumed to have a constant monomer concentration when monomer "reservoirs" are present. The gel effect is said to start when the droplets disappear and the particle monomer concentration decreases. This leads to an autoacceleration in rate as the viscosity within the particle increases. However, since all droplets are actually nucleated within a macroemulsion, their disappearance is a misnomer. The gel effect actually starts when the nucleated droplets no longer contain excess monomer. This leads to an autoacceleration in rate as the viscosity increases within the growing latex particle. This is usually modeled as a reduction in the termination rate constant. Because of the relatively small number of nucleated droplets in macroemulsions, their effect on the overall kinetics is minimal.

Miniemulsion particles originate as monomer droplets. They have a thermodynamic excess of



**Figure 5** Conversion-time curves of macroemulsion polymerizations of MMA for some runs shown in Figure 3. Recipes are based on the standard with variations only in the levels of surfactant. Run numbers for these curves are listed in Table I. The run chosen for  $[S]_0 = 0.04$  mol/L  $H_2O$  is KF20.



DEPENDENCE OF RATE ON SURFACTANT  
 MINIEMULSIONS


**Figure 6** Conversion-time curves of miniemulsion polymerizations of MMA for runs shown in Figure 4 where HD level is 5 g. Run numbers for these curves are listed in Table II. The run chosen for  $[S]_0 = 0.02$  mol/L  $H_2O$  is KF57.

monomer from the earliest stage. Although the monomer will diffuse between droplets and particles, there are no "reservoirs" of monomer available once nucleation is complete. Thus, the monomer concentration within the miniemulsion particles decreases throughout the reaction and the gel effect is a more gradual acceleration. In miniemulsions, the conversion time curves are concave upward early on, whereas macroemulsions usually have linear portions. The calculation of an  $\bar{n}$  is very error-prone in miniemulsion polymerizations because both the rate and the particle monomer concentration continually vary throughout the reaction.

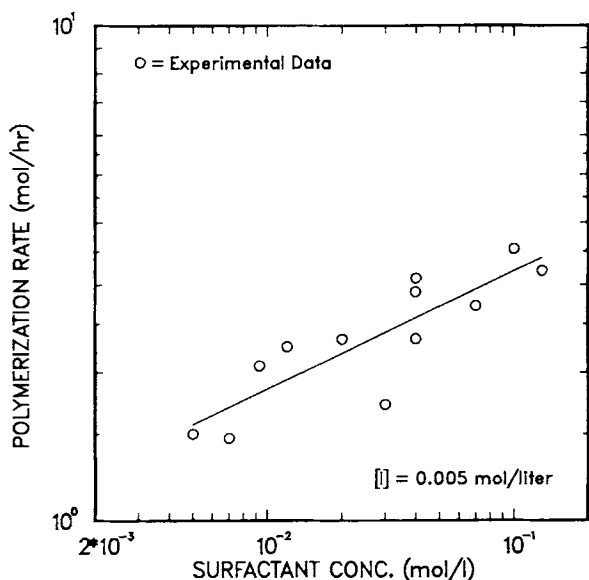
The rates of polymerization for the macroemulsion runs were calculated by averaging the slopes of the corresponding conversion time curves. Conversions between 10 and 45% were used since they approximately account for Interval II kinetics. The rates of polymerization are plotted on a log-log scale vs. surfactant in Figure 7. The linear least-squares (LLS) line is also shown and has a slope of 0.24

$\pm 0.13$ . There is a large amount of error in the slope estimate due to the calculation of polymerization rates from just a few conversion data points.

If the rates of polymerization are divided by the number of particles and the appropriate constants, the average particle radical number,  $\bar{n}$ , can be estimated. This value depends on the values used for  $k_p$  and  $[M]_p$ . The values used were  $k_p = 560$  L/mol/s and  $[M]_p = 5.91$  mol/L particle (65% by volume). The values calculated for  $\bar{n}$  are shown in Figure 8. At low surfactant concentrations, the particle number is small and the reaction follows SE Case II kinetics where  $\bar{n} = \frac{1}{2}$ . At higher concentrations, the particles are greater in number and smaller in size. The value of  $\bar{n}$  falls off from 0.5. This indicates that desorption plays a role in MMA macroemulsion polymerizations.

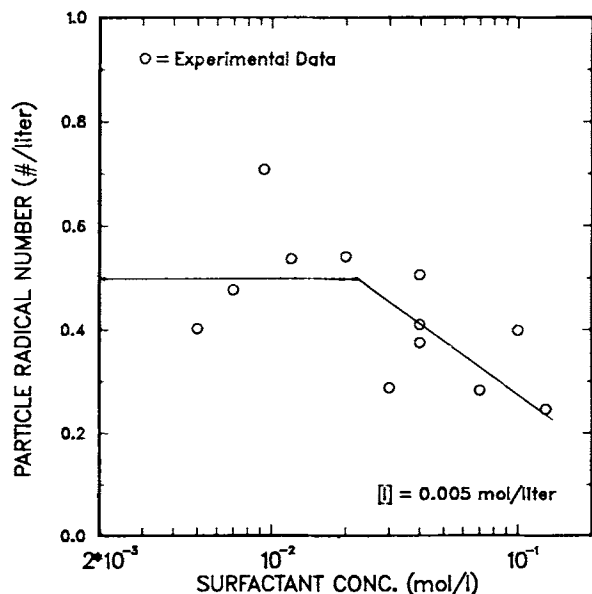
The corresponding points for miniemulsion polymerizations are more difficult to generate with reasonable accuracy. In miniemulsion polymerizations, there is not a linear portion of the conversion

POLYMERIZATION RATE DEPENDENCE ON SURFACTANT  
MACROEMULSION



**Figure 7** Polymerization rate of MMA macroemulsions at various levels of surfactant. Recipes are standard otherwise. Data points correspond to data in Figure 3. The line is the LLS fit to the data on the log-log scale.

RADICAL NUMBER DEPENDENCE ON SURFACTANT  
MACROEMULSIONS

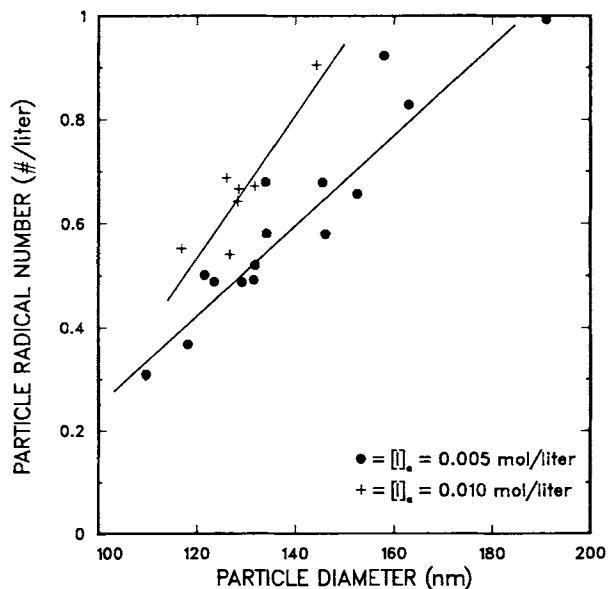


**Figure 8** Average particle radical number at conversions between 15 and 45% in MMA macroemulsion polymerizations at various levels of surfactant. Recipes are standard otherwise. Data points correspond to data in Figures 3 and 7.

curve. If the polymerization rate is averaged over 15–45% conversion, an estimate for  $R_p$  and  $\bar{n}$  can be obtained. The surfactant concentration is less meaningful in miniemulsion polymerizations. For this reason, the values of  $\bar{n}$  are plotted vs. final particle diameter, thereby eliminating the dependence on shear and HD. The values for  $\bar{n}$  are shown in Figure 9 for two levels of initiator. Unlike the macroemulsion polymerizations, the value for  $\bar{n}$  does not approach a limit of 0.5, but, instead, continues rising. The values used for  $k_p$  and  $[M]_p$  for the miniemulsions were 560 L/mol/s and 6.4 mol/L part (70% by volume).

The kinetics for miniemulsion polymerizations are different from macroemulsion kinetics. The miniemulsion particles must either have limited amounts of termination or high amounts of desorption. Direct comparison is difficult since the particle sizes in the two emulsions are different. The macroemulsion latex particles range from 78 to 132 nm, whereas the miniemulsion particles range from 110 to 190 nm. Scatter in the values for  $\bar{n}$  is largely due to the propagation of the errors in estimating  $R_p$  and  $N_p$ .

RADICAL NUMBER DEPENDENCE ON PART. DIAMETER  
MINIEMULSION



**Figure 9** Average particle radical number in MMA miniemulsion polymerizations as a function of particle diameter. Recipes are standard except for certain variations in HD, SLS, and sonication. The particle sizes are the RMC diameter of the final latex and the  $\bar{n}$  is at 15–45% conversion.

### 3.3. Effect of Cosurfactant

Cosurfactants are known to provide enhanced stability to submicron monomer droplets. Long-chain alkanes employed as cosurfactants are often referred to as swelling agents. An increase in the amount of swelling agent results in a decrease in the average monomer droplet diameter. This should correlate to a greater particle number and a higher rate. Figure 4 gives the effect of HD on the particle number for various concentrations of SLS. Although the number of particles increases with the amount of HD, there does not appear to be any interaction between the surfactant and cosurfactant. Unlike miniemulsions prepared with fatty alcohol cosurfactants, there is no optimum ratio of cosurfactant to surfactant when HD is used. This indicates that the formation of liquid crystals at the monomer-water interface is unlikely. The enhanced stability of miniemulsions with HD as cosurfactant is most likely due to the retardation of monomer diffusion. Stability of the final latex product is also affected, as discussed in a later section. It should be noted that due to the unknown amount of HD evaporation during the gravimetric measurements there are slight systematic errors in the percent conversion calculations and corresponding particle numbers.

### 3.4. Effect of Initiator

The Smith and Ewart theory provides a value of 0.4 for the order of the proportionality between particle number and initiator concentration. Experimental values that differ from this have been reported in the literature.<sup>12-17</sup> This proportionality is another distinguishing feature between macroemulsion and miniemulsion polymerizations. In miniemulsions, the upper limit for particle number is approached as the initiator is increased. This limit is the number of droplets. For macroemulsions, the upper limit is the number of micelles (assuming micellar nucleation) but is limited by ionic strength.

The number of monomer droplets in a miniemulsion is typically on the order of  $10^{17}$ /L. The number of micelles is on the order of  $10^{21}$ /L. When the initiator concentration is increased, miniemulsion polymerizations will reach a limiting particle number much sooner than will the corresponding macroemulsion. A limiting number of particles in macroemulsions would require an enormous amount of initiator, which is prohibited due to stability considerations.

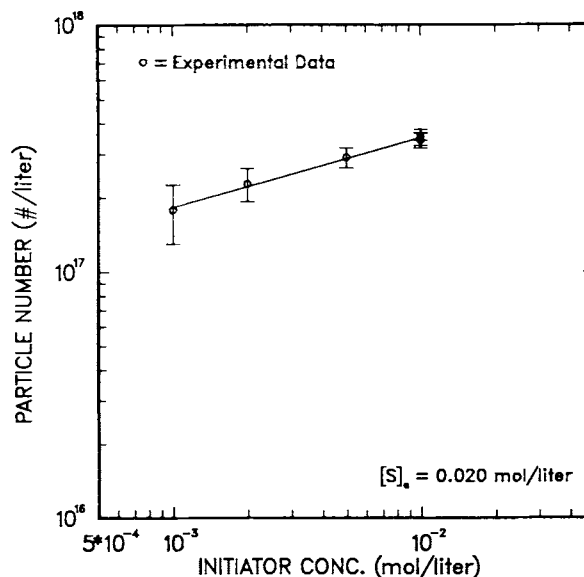
The proportionality of particle number to initiator concentration for macroemulsion and mini-

emulsion polymerizations are shown in Figures 10 and 11, respectively. All parameters other than initiator concentration are the same as those for the standard recipe. For the range of concentrations employed, the data indicate a linear relationship on the log-log scale between particle number concentration and initiator concentration. The slopes of these lines are  $0.28 \pm 0.05$  for the macroemulsion and  $0.11 \pm 0.05$  for the miniemulsion.

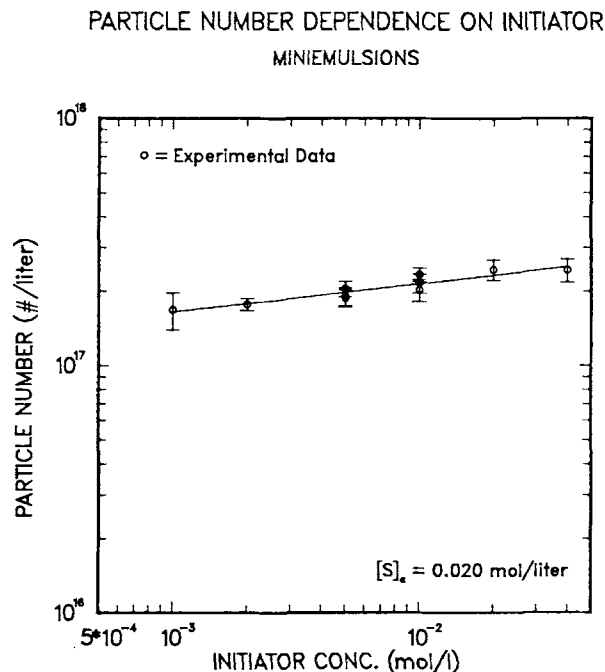
Delgado et al.<sup>19</sup> found the opposite relationship in his copolymerization work with vinyl acetate and butyl acrylate. For macroemulsions, the order was found to be 0.0, and for miniemulsions, 0.8. No justification was provided. The initiator was ammonium persulfate at concentrations ranging between 1.1 and 4.4 mM, lower than what is considered here. Choi et al.<sup>4</sup> found a linear relationship between initiator and particle number on the log-log scale for the miniemulsion polymerization of styrene. The slope of the LLS line was 0.37. Cetyl alcohol was used as cosurfactant, SLS for surfactant, and potassium persulfate as initiator.

The data presented here for miniemulsions seem to indicate a leveling off of particle number at high

PARTICLE NUMBER DEPENDENCE ON INITIATOR  
MACROEMULSIONS



**Figure 10** Particle number concentration vs. initiator concentration in macroemulsion polymerizations of MMA at 50°C. Other conditions are the same as the standard. Run numbers for the data points are given in Table I. Error bars are the 98% confidence intervals propagated from the variance of the particle-size measurement. The line is the LLS fit to the data.



**Figure 11** Particle number concentration vs. initiator concentration in miniemulsion polymerizations of MMA at 50°C. Other conditions are the same as the standard. Run numbers for the data points are given in Table II. Error bars are the 98% confidence intervals propagated from the variance of the particle-size measurement. The line is the LLS fit to the data.

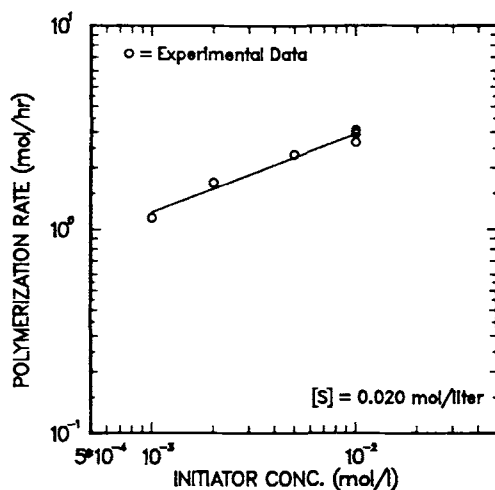
initiator concentrations. This is believed to correspond to the point in which all drops become nucleated. If this is true, the final particle number is the same as the initial droplet number. This could be verified if reliable drop size measurements were available. This indicates that, above a given level, the initiator concentration is of less importance in the miniemulsion polymerization than in the macroemulsion polymerization of MMA. Extrapolation of the two particle number vs. initiator curves to lower initiator concentrations would predict a crossover point. This would result in a miniemulsion polymerization having a higher particle number and a higher polymerization rate than those of the corresponding macroemulsion polymerization. The conversion times curves for the runs are available in Ref. 11.

The polymerization rates for the runs in Figures 10 and 11 were calculated by the method previously described. These rates are plotted vs. the initiator concentration in Figure 12 for both the mini- and the macroemulsion polymerizations. They both appear to be linear on the log-log scale within the range of initiator concentrations studied. The slopes of

the LLS line through the data points are  $0.39 \pm 0.15$  and  $0.40 \pm 0.10$  for the macroemulsion and miniemulsion, respectively. The miniemulsion data also appear to be approaching a limit at high initiator concentrations. However, due to statistical error in the data, this cannot be concluded for certain. The particle sizes for these runs range from 120 to 140 nm for miniemulsions and 106 to 140 for the macroemulsions.

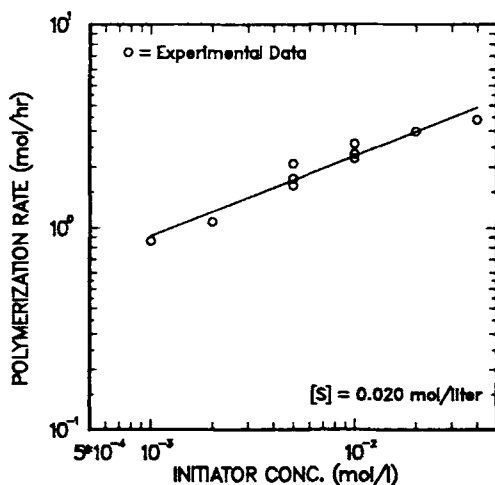
Chamberlain et al.<sup>3</sup> found a much different relationship in the miniemulsion polymerization of styrene. At initiator levels above 0.02 mol/L, they

POLYMERIZATION RATE DEPENDENCE ON INITIATOR  
MACROEMULSION



A.)

MINIEMULSION



B.)

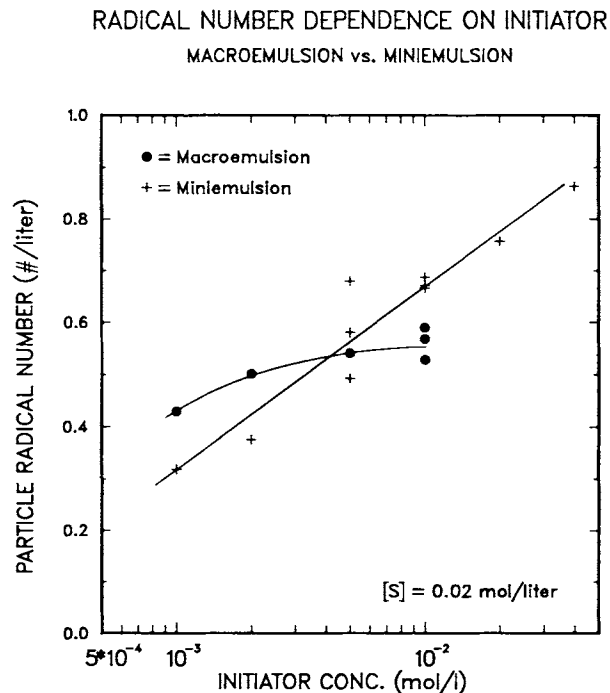
**Figure 12** Polymerization rates of MMA for (A) miniemulsions and (B) macroemulsions at various levels of initiator. Recipes are standard otherwise. Data points correspond to the data in Figures 10 and 11.

observed a sharp increase in the polymerization rate. This was postulated to be due to the inclusion of homogeneous nucleation in the polymerization. Particle-size distributions were used as supporting evidence.

The particle radical numbers for these data points were also calculated. These values are plotted vs. initiator concentration in Figure 13. The radical number rises with initiator concentration for both the miniemulsion and macroemulsion polymerizations. The macroemulsions do approach the 0.5 limit as per SE Case II kinetics. The miniemulsions do not appear to approach a limit. These differences could be exploited such that a miniemulsion will give a higher polymerization rate than will the corresponding macroemulsion, even at a lower particle number.

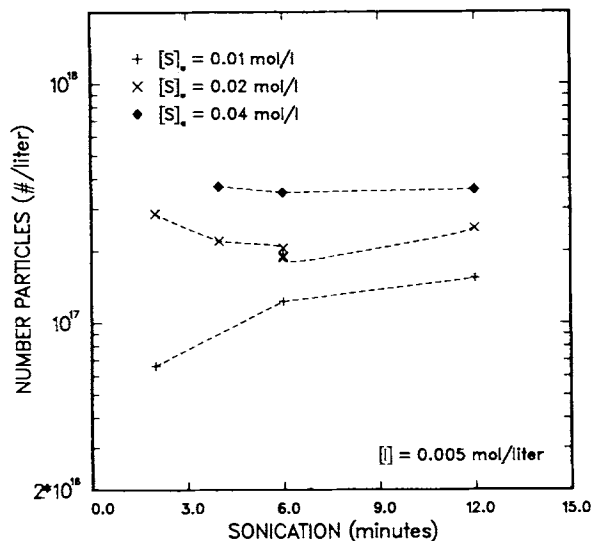
### 3.5. Effect of Sonication Intensity

The miniemulsion polymerizations discussed thus far all used the standard amount of sonication in their preparation; 6 min at 60% load on the 300 W dismembrator. It was found that this level of energy input would break up the droplets sufficiently to



**Figure 13** Particle radical numbers in MMA mini/macroemulsion polymerizations at various levels of initiator. Recipes are standard otherwise. Data points correspond to the data in Figures 10–12.

### PARTICLE NUMBER DEPENDENCE ON SONICATION MINIEMULSIONS

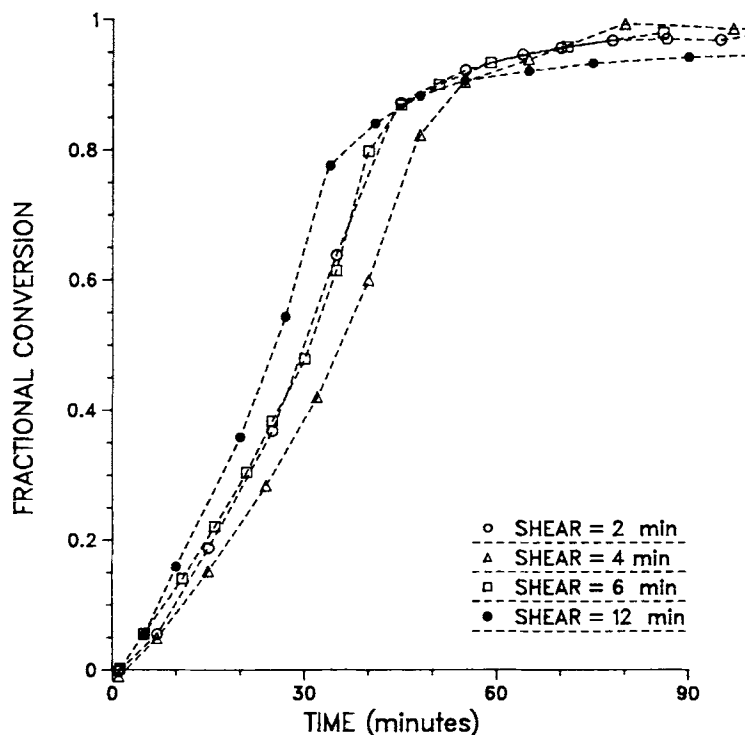


**Figure 14** Average particle number concentration in different MMA miniemulsion polymerizations at 50°C as a function of sonication intensity. Run numbers for the data points are provided in Table II. Recipes are standard except where noted. Radical concentration is for conversions between 15 and 45%.

provide a miniemulsion from the coarser macroemulsion.<sup>20</sup>

Figure 14 shows the variation of the particle number concentration at full conversion with minutes of sonication at 60% power for several concentrations of surfactant and two concentrations of initiator. It can be concluded from this figure that at high surfactant concentrations and low sonication times the presence of micellar or homogeneous-originated particles is likely. Figure 14 shows that at SLS concentrations of 0.02 and 0.04 the number of particles initially decreases with sonication and then begins to increase. This suggests that at low sonication levels the droplets are not decreased sufficiently in size to adsorb surfactant sufficient to eliminate the possibility of homogeneous or micellar particle nucleation. If the phenomenon observed was actually a second batch of particles late in the reaction, one would not expect the rate of polymerization to be higher early in the reactions, as observed in Figure 15. This possibility is therefore ruled out. To reduce the polydispersity of the particle size in miniemulsion polymerizations, there is a limit to the amount of surfactant that should be used. For 30% disperse phase MMA miniemulsions, this is near 0.02 mol/L aqueous.

DEPENDENCE OF RATE ON SONICATION  
MINIEMULSIONS ( $S = 0.02$ ,  $I = 0.01$ )



**Figure 15** Conversion-time curves for MMA miniemulsion polymerizations with various sonication intensities. Surfactant concentration is 0.02 mol/L  $H_2O$  and initiator concentration is 0.01 mol/L  $H_2O$ . Sonication times are 2 min = KF86, 4 min = KF85, 6 min = KF102, and 12 min = KF52. All other conditions are standard.

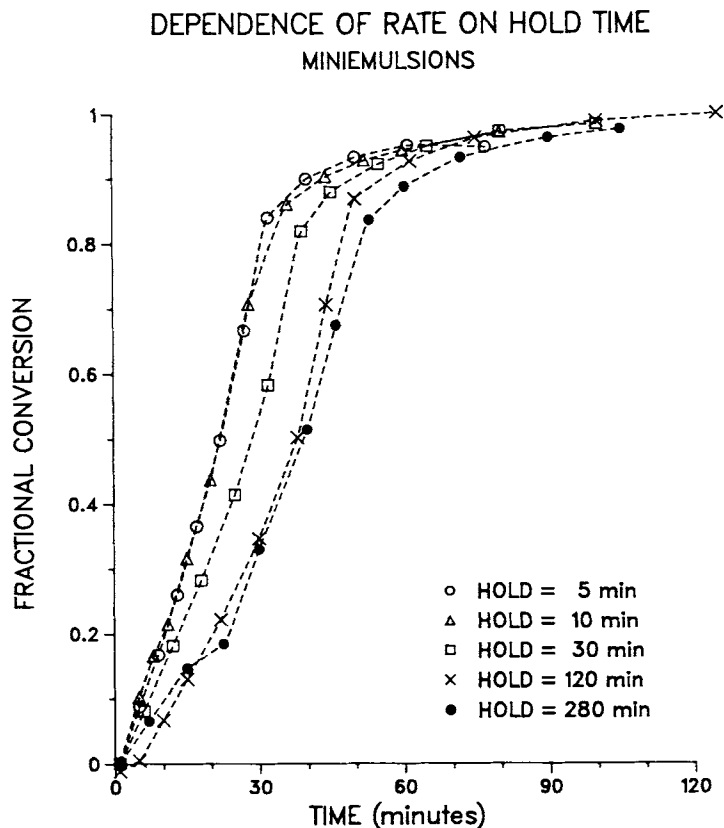
### 3.6. Effect of "Hold Time"

Miniemulsions experience both Ostwald ripening and coalescence after their preparation. This leads to a decrease in the number of droplets and an increase in their average diameter. These phenomena must inherently affect the polymerization of the emulsions. The miniemulsion polymerizations presented thus far were all initiated approximately 30 min after their preparation. The initial conditions for the polymerizations were therefore different from what would be experienced if initiation could proceed immediately after sonication. This has been reported to be important.<sup>3</sup>

To verify this theory, a revision was made to the batch emulsion polymerization apparatus. An outlet was installed on the bottom bell of the reactor. This outlet was connected with Tygon® tubing to another reactor bell having a similar outlet. This second bell housed the sonication device that rested on a fabricated lid that provided a closed system. A clamp on the Tygon tubing could be used to seal the two

bells off from each other. The emulsion was purged and presheared in the original reactor. It was then blown with nitrogen over to the second vessel (pre-purged with nitrogen) for sonication. After sonication, the miniemulsion was blown back over to the original vessel for polymerization. This new setup allowed initiation of polymerization within 5 min of sonication. For longer hold times (>30 min), the nitrogen purge was performed after sonication, just 30 min prior to initiation to avoid possible pre-polymerization due to sonication or UV absorption.

The conversion time curves for runs with hold times of 5, 10, 30, 120, and 280 min are shown in Figure 16. The difference between the 5 and 10 min conversion curves is negligible. This is expected since the period required for nucleation is longer than 5 min and ripening occurs during nucleation. The effect of hold time is therefore not seen due to the slow nucleation process. As the hold-up time approaches 2 h, there appears to be a limit in the amount of ripening. As predicted by droplet size measurements,<sup>20</sup> the difference between hold times



**Figure 16** Conversion-time curves for MMA miniemulsion polymerizations as a function of hold time. Run numbers corresponding to these hold times are 5 min = KF75, 10 min = KF73, 30 min = KF82, 120 min = KF76, and 280 min = KF81. Sonication time is 8 min and other parameters are per standard recipe.

of 120 and 280 min is negligible. The rate of polymerization approaches a lower limit as does the particle number.

There are several consequences of this ripening phenomenon: The first is the effect on reproducibility in batch miniemulsion polymerizations. If initiation is begun during the initial ripening period, the exact droplet distribution will be hard to reproduce. The resulting particle-size distribution will be affected. If initiation of polymerization is delayed until after 60 min when ripening and coalescence slows down, the reproducibility of the polymerization should be improved. The final state of the emulsion depends more on thermodynamics than on the amount of sonication.<sup>11</sup>

The ripening will also affect the results of continuous reactors. Here, the droplets are fed to the reactor immediately after sonication and can be nucleated before any noticeable amount of ripening or coalescence occurs. Consequently, the greatest number of droplets possible are nucleated. One would expect the particle numbers and rates ob-

tained in plug flow reactor (PFR) to exceed those in the corresponding batch miniemulsion polymerizations. A PFR would provide the smallest time between sonication of droplets and nucleation. The particle number in a continuous stirred tank reactor (CSTR) polymerization of a miniemulsion may have similar effects. It is more difficult to postulate in CSTRs since the residence time distribution (RTD) plays a major role. It is worth investigating experimentally. In continuous reactors, the dead time in the feed line between the sonicator and the reactor is a function of the feed rate. Thus, the feed rate affects both the feed conditions and the reactor residence time. Barnette and Schork found in the CSTR polymerization of MMA emulsions that twice as many particles were formed in the miniemulsion than in the corresponding macroemulsion, thus giving a much higher polymerization rate.<sup>2</sup>

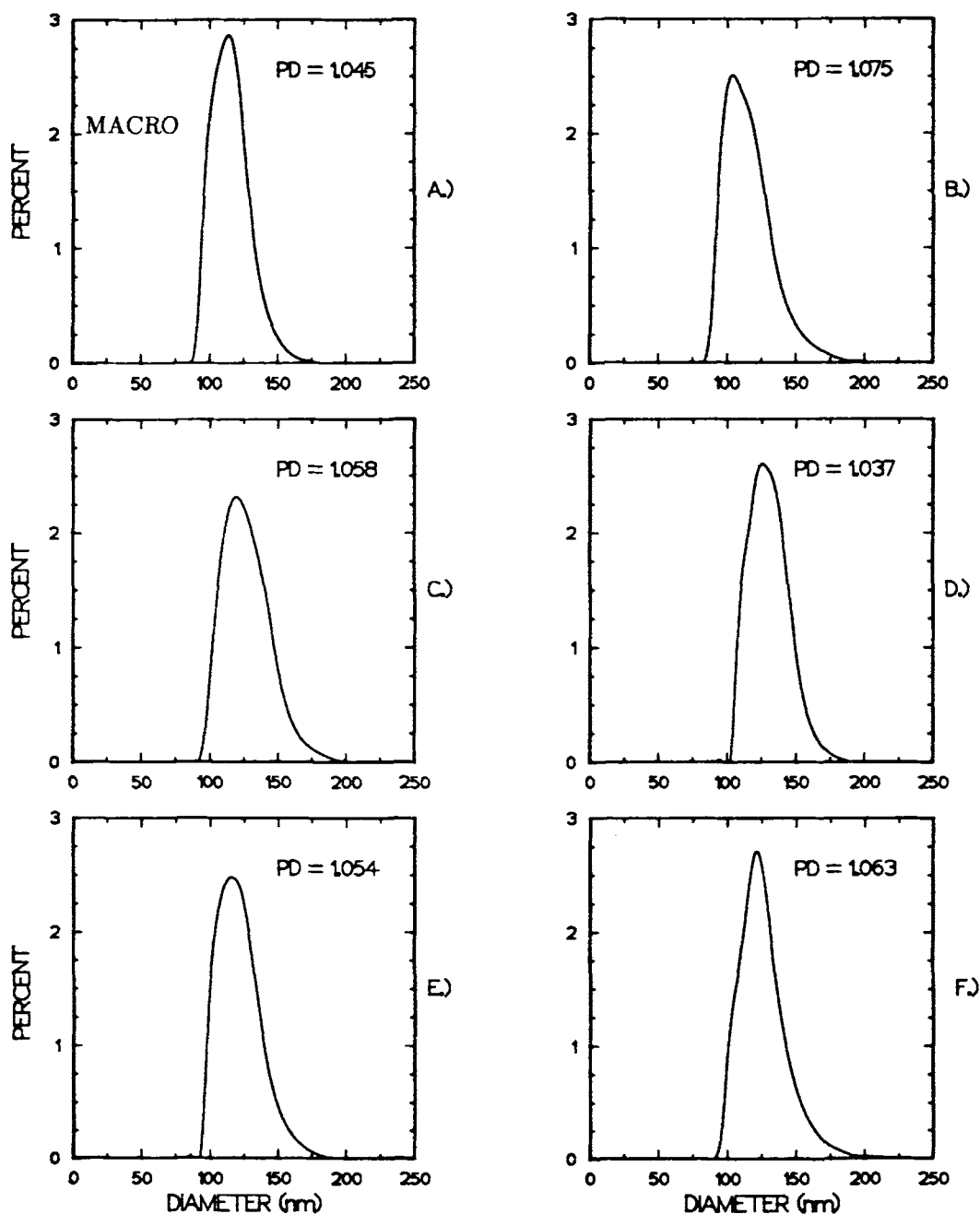
### 3.7. Particle-size Distributions

Barnette and Schork<sup>2</sup> showed that the particle-size distribution of a latex resulting from an MMA mini-

emulsion polymerization is indistinguishable from the corresponding macroemulsion polymerization latex. This work was done in a CSTR. The residence time distribution of the CSTR may have masked the differences in the two mechanisms. Delgado<sup>21</sup> reported the size distributions in the miniemulsion

copolymerization of vinyl acetate and butyl acrylate in a batch reactor. He found somewhat wider distributions in the miniemulsion latexes.

Data gathered in this work allow comparison of particle-size distributions for MMA miniemulsion polymerizations with the corresponding macro-

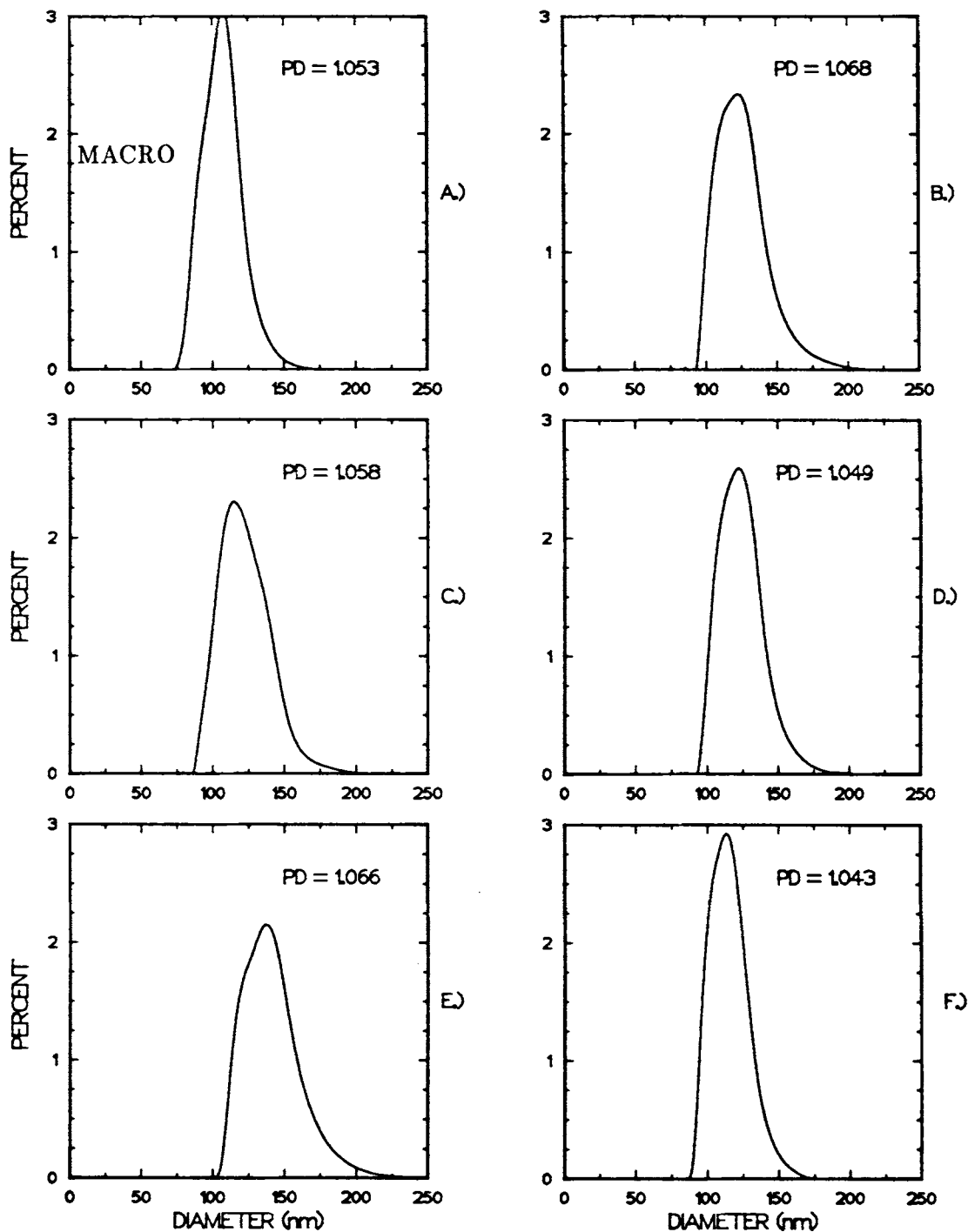


**Figure 17** Particle-size distributions of macroemulsion and miniemulsion latexes with  $[S]_0 = 0.02$  mol/L  $H_2O$  and  $[I]_0 = 0.005$  mol/L  $H_2O$ . (A) Macroemulsion KF11; (B) miniemulsion KF91: sonicate 2 min and 5 g HD; (C) mini-KF84: sonicate 4 min and 5 g HD; (D) mini-KF57: sonicate 6 min and 5 g HD; (E) mini-KF72: sonicate 12 min and 5 g HD; (F) mini-KF77: sonicate 8 min and 21 g HD.



emulsion polymerizations in a batch reactor. Figures 17 and 18 give a series of distributions of the miniemulsion polymerizations and the macroemulsion polymerization at two levels of initiator. The recipes

for the miniemulsion differed only by the amount of sonication and/or HD. Higher amounts of shear or HD should create a more monodisperse emulsion and, therefore, a latex that is more monodisperse.



**Figure 18** Particle-size distributions of macroemulsion and miniemulsion latexes with  $[S]_a = 0.02$  mol/L  $H_2O$  and  $[I]_a = 0.01$  mol/L  $H_2O$  and 5 g HD: (A) Macroemulsion KF10; (B) miniemulsion KF86: sonicate 2 min; (C) mini-KF85: sonicate 4 min; (D) mini-KF49: sonicate 6 min; (E) mini-KF82: sonicate 8 min; (F) mini-KF52: sonicate 12 min.

In these figures, it is observed that higher amounts of sonication gave narrower distributions. At high enough sonication, the polydispersity was actually lower than the corresponding macroemulsion. The polymerizations with the higher amount of initiator also gave the narrower distributions. It is expected that runs with lesser amounts of surfactant would also provide narrower distributions due to the avoidance of micellar nucleation. The major significance is that, through competitive growth, miniemulsions that have a polydispersity index of around 1.5 for the droplets, are converted to latexes with polymer particles that have a polydispersity index of only 1.05. The large droplets have a slightly higher radical concentration, but there are many more smaller particles. These small particles will therefore polymerize and consume monomer much more rapidly than will the large particles. The larger ones therefore give up the excess monomer to the smaller ones.

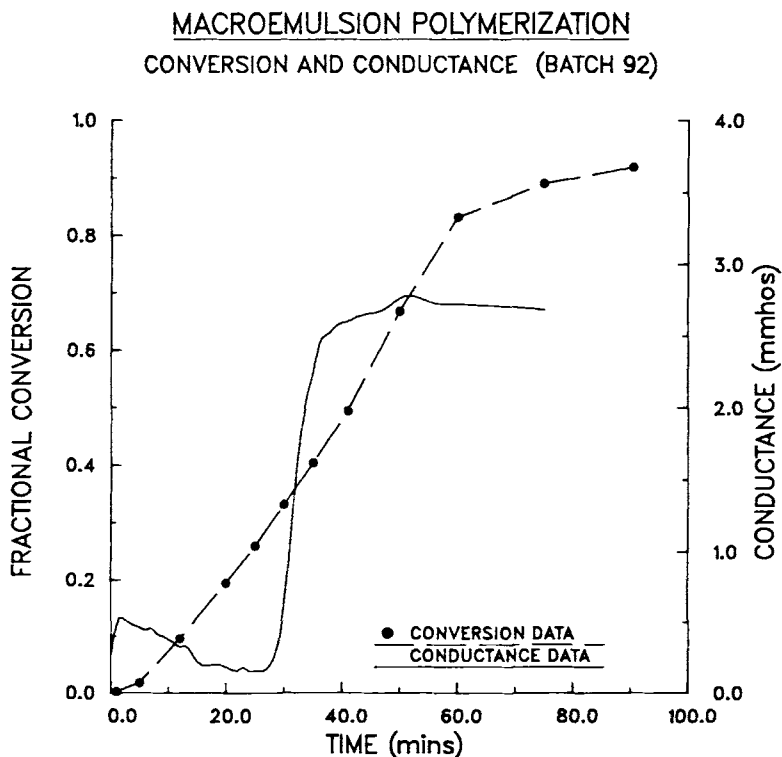
### 3.8. Conductance during Polymerization

The conductance measurements taken during emulsion preparation provide insight on emulsion stability.<sup>20</sup> To take these measurements a step fur-

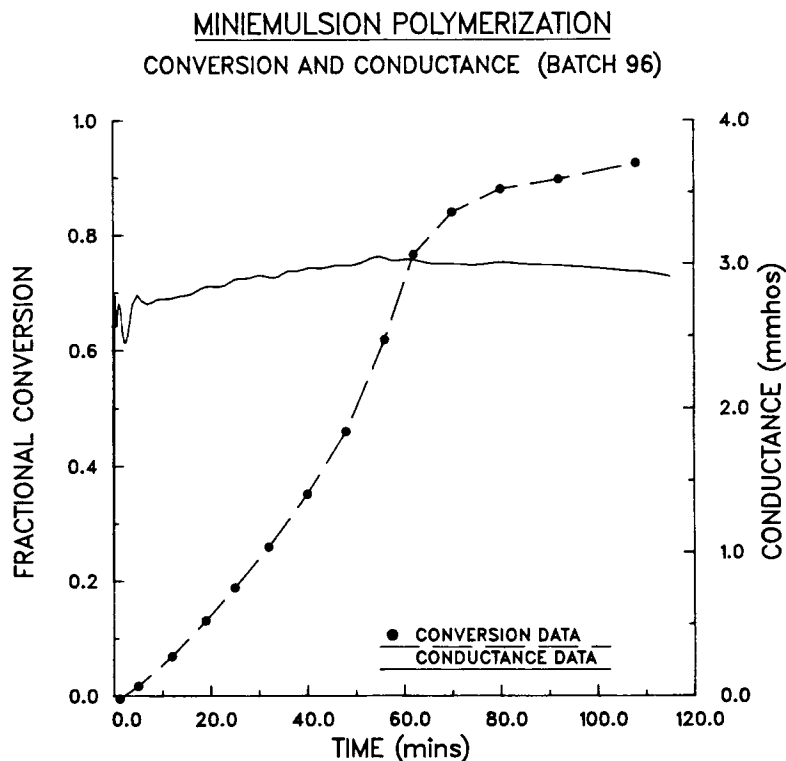
ther, the conductance was measured during polymerization. To provide this measurement, a recirculation loop was installed on the reactor. A dip-style conductance probe was not feasible due to the potential of coagulation and the interference of the stainless-steel coil and dip tubes on the conductance.

The recirculation loop was installed using silicone tubing and an in-line flow conductance probe. The reactor contents were drawn from the bottom of the bell and returned to the top with a peristaltic pump. The residence time in this loop was minimized. The tubing itself was found to partially inhibit the reaction; hence, the conversion-time data are not otherwise useful.

The conversion-time curve and conductance curve are plotted on the same graph for comparison purposes. Figure 19 provides the data for macroemulsion run KF92, and Figure 20, for miniemulsion run KF96. Reproducibility was verified (but not shown) and deemed adequate for the macroemulsion. The conductance for the macroemulsion polymerization immediately increased upon the addition of initiator at the start of the reaction. This was followed by a decrease in conductance as particles were formed. However, at approximately 30% conversion, the conductance increased dramatically.



**Figure 19** Conductance of an MMA macroemulsion during polymerization at 50°C. Run number is KF92.



**Figure 20** Conductance of an MMA miniemulsion during polymerization at 50°C. Run number is KF96.

It peaked out and then decreased at a low rate. It is believed that the increase in conductance corresponds to the disappearance of excess monomer and a desaturation of the aqueous phase. A model developed in conjunction with this work shows that the droplets (although nucleated) undergo a sudden shrinking at about 30% conversion.<sup>11</sup> This matches the conductance observations quite well.

The measured conductance of a miniemulsion during polymerization was quite different. The conductance increased sharply immediately after addition of initiator to the reactor. The conductance then increased at a much lower rate, followed by a slow decrease after peaking at approximately 50% conversion. This curve is quite different from the macroemulsion curve. It shows that in miniemulsions there is little change in surface characteristics. There is also no sudden shrinking of droplets to provide monomer to particles. Since approximately all droplets are believed to be nucleated, they all grow and provide a sink for the monomer. This is direct evidence of droplet nucleation occurring instead of micellar or homogeneous nucleation.

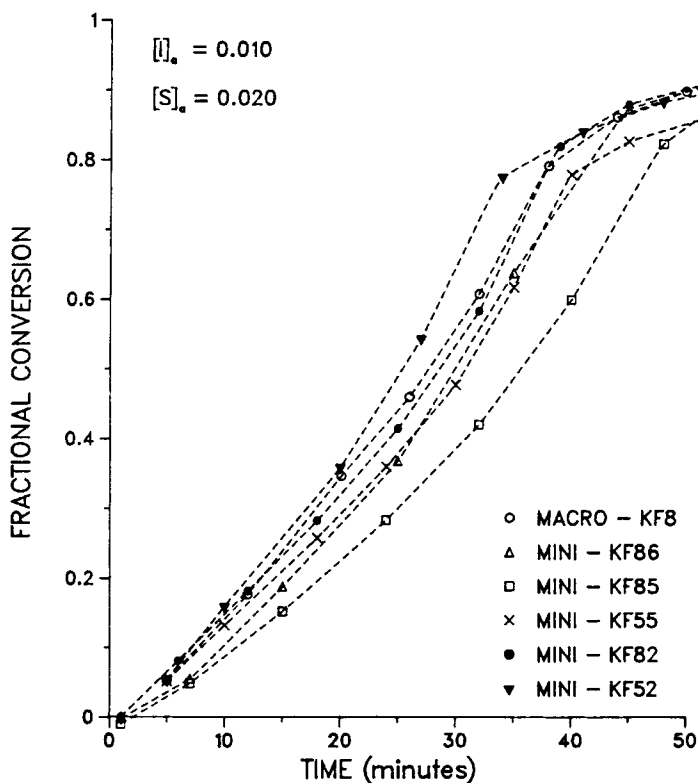
Although only one macroemulsion and one miniemulsion recipe were tested, they reveal interesting facts about the polymerizations: The measurements

were instantaneous and easy to make. Advancement of this method and further work would help provide insight into the different mechanisms in macroemulsions vs. miniemulsions. It may also serve to give an indication of the end of Interval II in macroemulsion polymerizations.

### 3.9. Mini- vs. Macroemulsion Polymerization

One objective of this work was to determine the conditions under which miniemulsions polymerize faster than do the corresponding macroemulsion. There have been reportings of this<sup>2,22</sup>; each used HD as the cosurfactant. However, most miniemulsions seem to polymerize at a lower rate than that of the corresponding macroemulsion. This appears to be a direct consequence of the number of particles produced. The data presented here provide an opportunity for a comparison.

The conversion-time curves reveal several interesting traits: Figure 21 shows the effect of increasing the length of sonication. The run with only 2 min of sonication was slightly slower than was the macroemulsion curve. As sonication was increased, the rate of polymerization decreased, but eventually began to increase until at 12 min of sonication the

EMULSION POLYMERIZATION  
 MINI vs MACRO


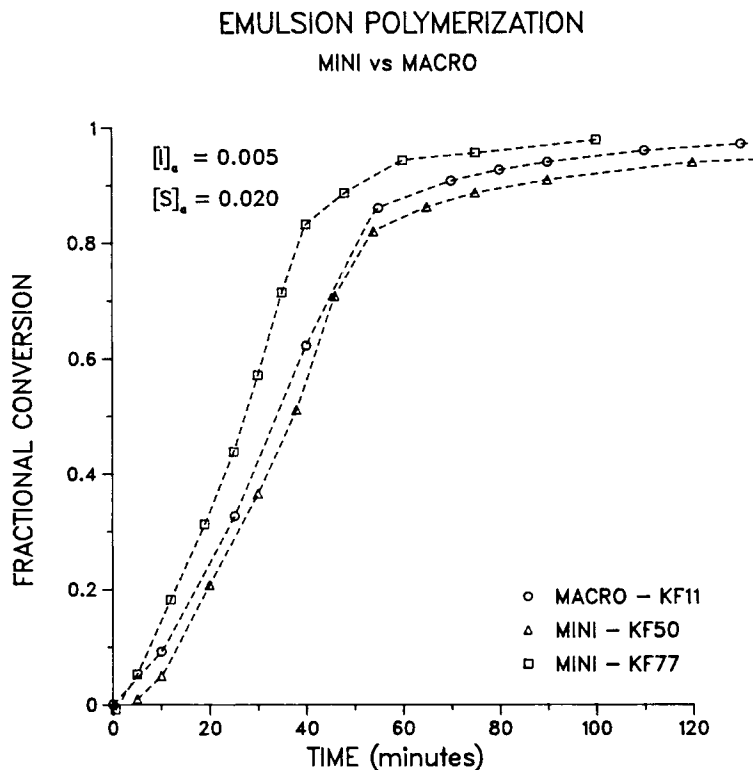
**Figure 21** Mini- vs. macroemulsion polymerization conversion-time curves; effect of sonication. Recipes are standard except run amount of sonication and  $[I]_0 = 0.010$  mol/L  $H_2O$ . Sonication times are KF8 = 0 min, KF86 = 2 min, KF85 = 4 min, KF55 = 6 min, KF82 = 8 min, and KF52 = 12 min.

polymerization rate for the miniemulsion slightly exceeded that for the corresponding macroemulsion. This indicates that at low levels of sonication there are still micelles present. As the length of sonication increases, all micelles eventually disappear. At this point, the rate reaches a minimum. As sonication intensity was further decreased, smaller droplets in larger number were created. The particle number rose and the polymerization rate increased. One would expect the particle-size distributions of the low sonication runs to be much wider due to two mechanisms of particle formation. Experimental evidence of this was reported earlier in this work.

The particle numbers calculated for this set of runs are lower for all the miniemulsions as compared to the macroemulsion polymerization. Even though run KF52 had a rate exceeding KF8, the particle number was actually lower ( $2.9 \pm 0.2 \times 10^{17}$  vs.  $3.4 \pm 0.2 \times 10^{17}$ ). This indicates that the monomer con-

centration or the radical number must be higher for the miniemulsion than for the macroemulsion. This is also evident in comparing run KF77 with KF11. The particle numbers were the same ( $2.9 \times 10^{17}$ ), but miniemulsion run KF77 had a rate that exceeded the polymerization rate for macroemulsion KF11 (see Fig. 22).

The possible miniemulsion-to-macroemulsion comparisons are too numerous to reproduce here in graphic form. For this reason, conclusions are listed below. However, it must be noted all the runs presented had a hold time of 30 min. Comparison of runs with less hold time leads to additional conclusions. Figure 23 shows the conversion-time curves for miniemulsion run KF75 and macroemulsion run KF10. The hold time on the miniemulsion was 10 min. Here, the miniemulsion rate exceeded the macroemulsion rate. The particle numbers were not statistically different. Evidently, miniemulsions can



**Figure 22** Mini- vs. macroemulsion polymerization conversion-time curves. Recipes are standard except for KF77 = 8 min sonication and 21 g of HD, and KF50 = 6 min sonication and 10 g of HD.

obtain higher rates than can macroemulsions under the right conditions. The reason for this is a higher particle radical concentration in miniemulsions.

The data presented above, as well as other unreported results, allow the following conclusions:

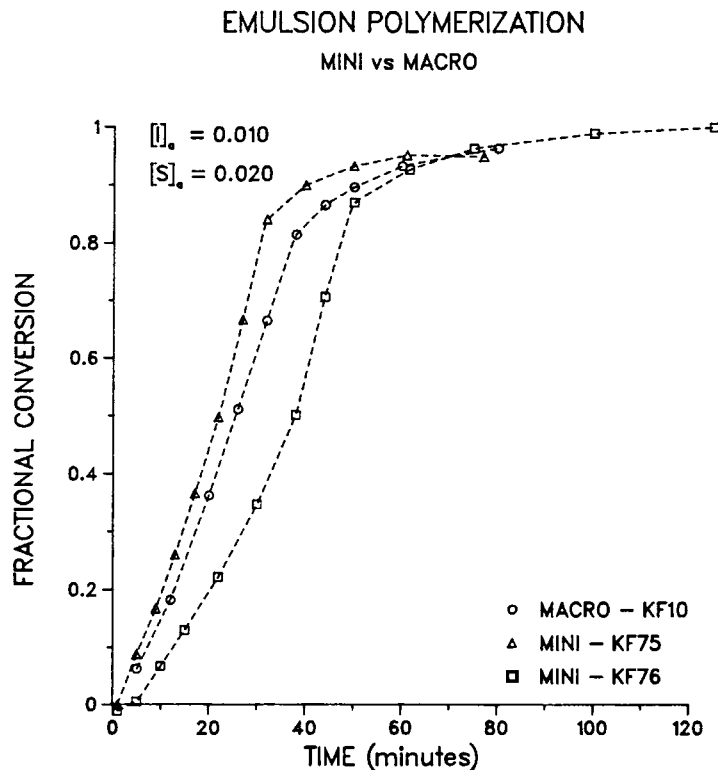
- Miniemulsions can polymerize faster than can corresponding macroemulsions under one or more of the following conditions:
  - Very high amounts of sonication with low amounts of surfactant;
  - High levels of cosurfactant;
  - Low hold times in a batch reactor, or
  - In a PFR (and CSTRs) where nucleation occurs immediately after sonication.
- The monomer concentration and/or radical number can be higher in miniemulsion particles.
- To avoid broad particle-size distributions, avoid low sonication levels that allow micellar nucleation to occur.

- Although sonication is employed in the preparation of an emulsion, it does not guarantee the sole locus of nucleation is the monomer droplets at high surfactant levels, (i.e.,  $> 0.02$  mol/L  $H_2O$ ).

### 3.10. Latex Stability

Theoretically, all droplets in a macroemulsion are nucleated into polymer particles. The low concentration ( $1 \times 10^{13}$ ) vs. micellar particles ( $1 \times 10^{17}$ ) results in no influence on the measured particle-size distributions. However, even at this low concentration (0.01% by number but higher in mass), they may have a destabilizing influence on the latex. Large particles act as nucleating sources for flocculation or coagulation. Small particles will preferentially coagulate with large ones.<sup>23,24</sup> Therefore, a truly monodisperse latex would be the most stable, everything else being equal.

Several techniques can be used to analyze stabilities of prepared latexes. These include shelf life, titration, and high-speed shearing. To provide a valid



**Figure 23** Mini- vs. macroemulsion polymerization; effect of low hold time on conversion-time curves. Run KF75:  $[S]_0 = 0.02$  mol/L  $H_2O$ .  $[I]_0 = 0.01$  mol/L  $H_2O$ , sonication = 8 min, and hold time = 5 min; run KF76: hold time = 120 min; run KF10: macro.

comparison of stability, as many parameters as possible should be the same. These include surfactant concentration, initiator concentration, monomer concentration, final conversion, and particle size. Here, two emulsions were studied via titration. Macroemulsion run KF24 and miniemulsion run KF73 used the same amount of surfactant and produce approximately the same size particles: 118 nm for KF24 and 122 nm for KF73.

Titration of a latex with acetone or an  $Al_2(SO_4)_3$  solution causes it to coagulate once a critical concentration is reached. The two latexes here were titrated by both acetone and a 5 g/L solution of  $Al_2(SO_4)_3$ . The results were qualitative. Both emulsions appeared to break about the same time with both the acetone and  $Al_2(SO_4)_3$ . Further addition of coagulating agent simply resulted in dilution of the latex.

The results of this test indicate the lack of difference in surface characteristics between the macroemulsion and miniemulsion polymerization products. A difference would be likely if the cosurfactant in the miniemulsion formed a liquid crystal on the surface of the particle as expected with long-chain

alcohol cosurfactants. It was postulated that HD provides stability via diffusional limitation. These experiments agree with this.

A second stability test was performed using a Warring blender. Here, 400 g of fully converted latexes KF30 and KF69 were each sheared at high speed for 5 min. The increases in volume over time were found to be approximately equal for the two emulsions. The final volume was almost twice the original. This increase was due to foaming of the latex. After allowing the sheared latexes to settle, the macroemulsion product had partially coagulated. The miniemulsion latex was still stable. The test points toward a difference in the two types of latex. The miniemulsion latex does not have the large polymerized droplets to cause stability problems. This is a definite advantage over the macroemulsion.

#### 4. SUMMARY

There are substantial amounts of data presented in the paper. The analysis of the data has followed numerous paths. It is good to summarize the key find-

ings in the area of mini/macroemulsion polymerization.

Particle nucleation has been shown to follow two distinguishable mechanisms. Conductance during polymerization is a direct consequence of this. This difference leads to a difference in the importance of initiator and surfactant on the formation of new particles. Droplet nucleation was shown to induce a limit on the number of particles in the reactor. Particles nucleated from droplets were observed to have higher radical numbers than that of the macroemulsion particles. There is no true linear portion of the conversion-time curve for the miniemulsion polymerization. Miniemulsions will polymerize faster than will the corresponding macroemulsions under certain criteria.

Cosurfactant (HD) was shown to greatly enhance the stability of small droplets and therefore increase particle numbers. There is not an "ideal" ratio between HD and SLS. There are limits on permissible surfactant concentrations to avoid micellar and/or homogeneous nucleation. Two simultaneous nucleation mechanisms result in a wide particle-size distribution. Miniemulsion age was shown to affect the polymerization and thus suggest higher particle numbers can be obtained in continuous reactors. The hold time plays a key role in reproducibility of nucleation.

Miniemulsions seem to produce latexes that are more shear stable than are macroemulsions. This could lead to a commercial advantage. Tailoring the desired particle size distribution may also be easier in miniemulsion polymerizations if other nucleation regimes can be avoided. Several factors still need addressing in this area. These include the effect of monomer concentration on nucleation and the use of a PFR to vary hold time and to look at droplet swelling via polymerization of all droplets into particles since reliable droplet size measurements have been difficult to obtain.

## REFERENCES

1. W. V. Smith and R. H. Ewart, *J. Chem. Phys.*, **16**, 592 (1948).
2. D. T. Barnette and F. J. Schork, *Chem. Eng. Commun.*, **80**, 113-125 (1989).
3. B. J. Chamberlain, D. H. Napper, and R. G. Gilbert, *J. Chem. Soc. Faraday Trans. I*, **78**, 591-601 (1982).
4. Y. T. Choi, M. S. El-Aasser, E. D. Sudol, and J. W. Vanderhoff, *J. Appl. Polym. Sci.*, **23**, 2973-2987 (1985).
5. D. P. Durbin, M. S. El-Aasser, G. W. Poehlein, and J. W. Vanderhoff, *J. Appl. Polym. Sci.*, **24**, 703-707 (1979).
6. J. Delgado, M. S. El-Aasser, C. A. Silebi, and J. W. Vanderhoff, *J. Polym. Sci. Polym. Chem. Ed.*, **24**, 861-874 (1986).
7. V. S. Rodriguez, PhD Thesis, Lehigh University, 1988.
8. R. C. Dewald, L. H. Hart, and W. F. Carrol, Jr., *J. Polym. Sci. Polym. Chem. Ed.*, **22**, 2931-2939 (1984).
9. P. L. Tang, PhD Thesis, Lehigh University, 1991.
10. K. Fontenot and F. J. Schork, *Polym. React. Eng.*, to appear.
11. K. Fontenot, PhD Thesis, Georgia Institute of Technology, 1991.
12. J. L. Gardon, *J. Polym. Sci. Part A-1*, **6**, 643-664 (1968).
13. J. G. Brodnyan, J. A. Cola, T. Konen, and E. L. Kelley, *J. Colloid Sci.*, **18**, 73-90 (1963).
14. R. M. Fitch and C. H. Tsai, in *Polymer Colloids*, R. M. Fitch, Ed., Plenum Press, New York, 1971, pp. 73-102.
15. F. K. Hansen and J. Ugelstad, in *Emulsion Polymerization*, I. Piirma, Ed., Academic Press, New York, 1982, pp. 51-93.
16. F. K. Hansen and J. Ugelstad, *Makromol. Chem.*, **180**, 2423-2434 (1979).
17. N. Sutterlin, in *Polymer Colloids II*, R. M. Fitch, Ed., Plenum Press, New York, 1980, pp. 583-597.
18. F. K. Hansen and J. Ugelstad, *J. Polym. Sci. Polym. Chem. Ed.*, **17**, 3047-3067 (1979).
19. J. Delgado, M. S. El-Aasser, C. A. Silebi, and J. W. Vanderhoff, *J. Polym. Sci. Polym. Chem. Ed.*, **28**, 777-794 (1990).
20. K. Fontenot and F. J. Schork, to appear.
21. J. Delgado, PhD Thesis, Lehigh University, 1987.
22. J. Ugelstad, H. Flagstad, F. K. Hansen, and T. Ellingsen, *J. Polym. Sci.*, **42**, 473-485 (1973).
23. J. Th. G. Overbeek, in *Colloid Science*, H. R. Kruyt, Ed., Elsevier, Amsterdam, 1952, Vol. 2, p. 290.
24. M. von Smoluchowski, *Z. Phys. Chem.*, **92**, 155 (1917).

Received October 4, 1991

Accepted October 28, 1992